MECHANICS OF EROSION

Shreyansh Patel

Northeastern University

360 Huntington Avenue, Boston, MA-02115

patel.shre@husky.neu.edu

1. Introduction

Erosive wear of metal surfaces is a difficult process to examine and understand. It not only involves a stress system of complex nature, large plastic deformations and high strain rates but also involves significant micro structural changes in the surface layer. Thus, it is not surprising that though, study on the phenomena of erosion has been going since the beginning of the century, still there is no universally accepted predictive model or mechanism for erosion. However, a number of erosive wear models have been proposed.

The major problem with the models is those that are more rigorously derived offer little possibility for experimental validation. In these models, the theoretically derived predictions of the erosion rate encompass a large number of parameters, both mechanical and physical properties, often experimentally difficult to determine under the conditions pertaining to erosion. Simple models tend to indicate the primary importance of one or more mechanical properties. However, there is again the problem of how to define and measure these properties under the stains and strain rates typical to erosion. Due to impossibility to generate the conditions, most of the researchers have used properties measured under more conventional conditions.

Though there are many aspects to erosion, through this report an attempt has been made to review the erosive wear phenomena occurring on metals, by studying the works in this field over this long period of time. In the direction to do so, various major wear models proposed are studied and compared with each other. Then single particle effect and the fluid effect for the erosion are discussed. Lastly, the phenomenon of erosion-corrosion is looked upon.

2. Wear Models

Ian **Finnie**[1] is the first person to propose a wear model. The model considers that the amount of surface material eroded by solid particles in a fluid stream depends on the conditions of the fluid flow and on the mechanism of material removal. It likens the particle to the cutting edge of a tool which moves into the specimen surface causing deformation and removal of the material (figure 1).

Considering Q, as the volume of material removed by grains of mass M with a velocity V and α as the angle at which the particle strikes the surface i.e. same as the angle of jet to the surface, we get

$$Q \approx \frac{MV^2}{8p}\left[\sin 2\alpha - 3\sin^2\alpha\right] \quad \alpha \leq 18.5° \tag{1}$$

$$Q \approx \frac{MV^2}{8p}\cos^2\alpha \quad \alpha \geq 18.5° \tag{2}$$

where value for α =18.5°, is the angle of jet at which the particle stops coming out of the material.
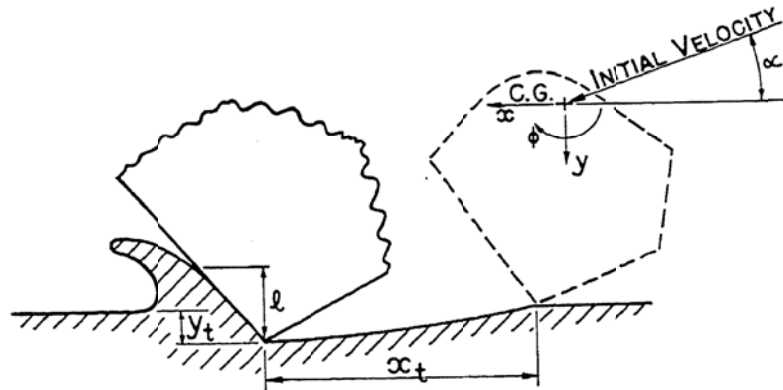

Figure 1 Idealized picture of abrasive grain striking a surface and removing material for Finnie's model.[1]

The model given above has a limitation that for angles above say 45°, it greatly underestimates the weight loss. It also seems that the above equation is good for

ductile specimens at small angle of attack. However, the relationship gives no erosion for impact angle of 90°.

To account for these discrepancies of normal impact and for brittle materials, **Bitter**[2][3] suggested a model, stating that this type of erosion comprise of two types of wear. One caused by repeated deformation during collision, eventually resulting in breaking loose of a piece of material. Other caused by cutting action similar to that used by Finnie.

The deformation wear found is given by:

$$W_D = \frac{1}{2} \frac{M(V \sin \alpha - K)^2}{\varepsilon} \qquad (3)$$

where W_D is the erosion in volume loss, M and V are the total mass and velocity of the impinging particle, α is the impact angle, K is a constant calculated from mechanical and physical properties and ε represents the energy needed to remove unit volume of the material for the body surface.

Cutting wear is given by:

$$W_{C1} = \frac{2MC(V \sin \alpha - K)^2}{\sqrt{V \sin \alpha}} \left(V \cos \alpha - \frac{C(V \sin \alpha - K)^2}{\sqrt{V \sin \alpha}} \rho \right) \qquad \alpha \leq \alpha_0 \qquad (4)$$

$$W_{C2} = \frac{1}{2} \frac{\left[V^2 \cos^2 \alpha - K_1 (V \sin \alpha - K)^{3/2} \right]}{\rho} \qquad \alpha \geq \alpha_0 \qquad (5)$$

where total wear at every instant is either

$$W_t = W_D + W_{C1} \qquad OR \qquad W_t = W_D + W_{C2} \qquad (6)$$

Here, α_0 is the angle at which the velocity component or the particle parallel to surface becomes zero, W_{C1} and W_{C2} are the cutting wear for angle conditions given, K_1 and C are parameters that depend on the physical properties of the surface material, and ρ is cutting wear factor.

From the a Bitter's model is seen that deformation wear accounts for the erosion at 90° in ductile materials and it is this wear that is not accounted by Finnie. Thus this model shows that for ductile materials maximum wear occurs at lower impact angles and for brittle and higher impact angles near to 90°.

Though Bitter's model found the erosion at normal angle, the theoretical work is exhaustive and intricate, as is accounts for both elastic and plastic properties for particle and specimen material. This complexity is removed by **Neilson-Gilchrist** [4] model. This model uses simple cutting and deformation wear constants φ and ε compared to four parameters in Bitter's model. The model is given as:

$$W = \frac{1}{2}\frac{MV^2\cos^2\alpha\sin n\alpha}{\phi} + \frac{1}{2}\frac{M(V\sin\alpha - K)^2}{\varepsilon} \qquad \alpha \le \alpha_0 \tag{7}$$

$$W = \frac{1}{2}\frac{MV^2\cos^2\alpha}{\phi} + \frac{1}{2}\frac{M(V\sin\alpha - K)^2}{\varepsilon} \qquad \alpha \ge \alpha_0 \tag{8}$$

where α_0 is the angle at which the velocity component or the particle parallel to surface becomes zero, W is the erosion produced by mass M of the particles at velocity V, and K is the velocity component normal to the surface below which no erosion takes place.

Though the number of parameters has been reduced here, the ratio φ/ε is very complex to obtain for each material.

Hutchings[5] observed that debris eroded from the specimen at normal incidence were flat, platelet form and jagged edges, unlike those formed at shallow angles. The platelet mechanism of erosion differs from cutting process; here platelets are formed at normal impingement detaches from the surface only after many cycles of plastic deformation. It uses the criterion of critical strain 'ε_c' i.e. removal of the fragment for the material maximum plastic strain within the fragment is reached on repeated impacts. The model is given as:

$$E = 0.033 \frac{\alpha \rho \sigma^{1/2} \upsilon^3}{\varepsilon_c^2 P^{3/2}}$$

(9)

where σ is the density of the impact particles, v is impact velocity, P pressure, α is the fraction of volume of indentation.

This model though simple does not consider the effect of strain hardening due to repeated impacts, also the ratio α and ε_c are to be measured experimentally.

Sundararajan's[6] model combines the concept of localization of plastic deformation leading to lip/platelet formation and generalized energy absorption relations valid for all impact angles and any shape of the eroding particles. The model is given as:

$$E = L^3 \left(\frac{\Delta \varepsilon_p}{\varepsilon_c} \right)^x$$

(10)

where L is the length of the plastic zone, $\Delta\varepsilon_p$ average strain per impact, and ε_c is the critical strain.
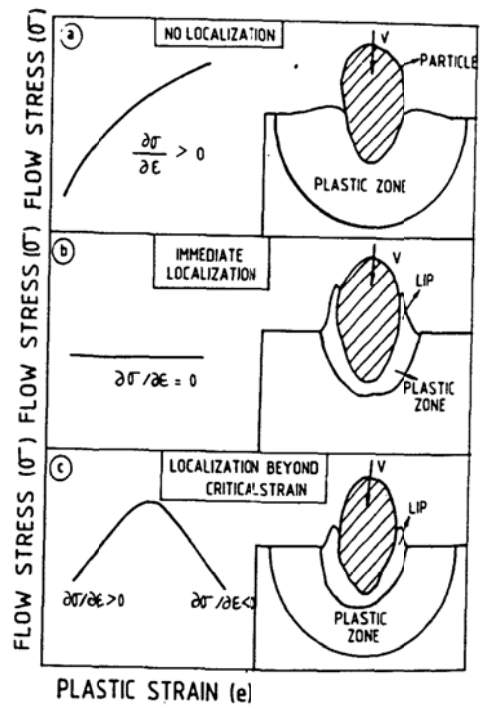

Figure 2 shows the influence of strain hardening capability of material on its susceptibility of localization during particle impact.[6]

6

$$L = rC\left(\frac{\sigma V^2}{k_0}\right)^a \qquad OR \qquad L = \alpha W \tag{11}$$

In the above equation α is the proportionality constant, W is width of the crater, σ is particle density, C and a are parameters dependent on particle shape.

Thus, the given model gives the erosion for particle of any shape. But, the model is quite complex involving many parameters. Also, some researchers consider that the output does not match with experimental output convincingly.

3. Particle Impact

There are many particle parameters involved for the study of erosive wear by particles entrained in liquid jet. Studying the effect of each independently will not give good results as they are inter-dependent, but studying them all together is almost impossible due to the complexity involved. Some of these are discussed below:

3.1 Particle size

It seems obvious that with decrease in erodent particle size, there will be decrease in erosion rate. But it accompanies with it significant changes in slurry flow conditions and particle motion which can mask the nature of particle size effect.[11]

This can be shown that even if the macroscopic properties like jet velocity, mass concentration etc. are kept constant and only the size of the particle is varied, the experimental conditions will change in a manner uncontrollable. For example, as the particle size is reduced, liquid drag on the particles becomes increasingly dominant so that small particles more completely conform to the movement of the bathing liquid that the large particles. This

results in reductions in particle impact velocities, particle impact angles and impact frequency. Thus it is found that doing experiments for different particle sizes under same conditions is practically impossible.

The experimental results showing the effect of particle size on erosion are shown in figure 3 and 4 as the function of peak erosion rate and the angular erosion limit. The results shown here are as expected; rate of wear increases with the increase in nominal particle size.
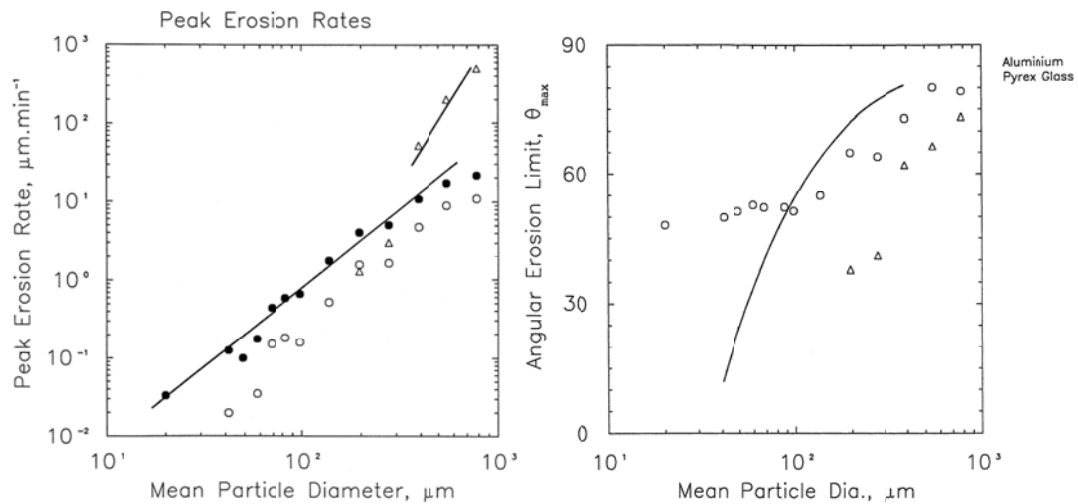

Figure 3 and 4 Variation of peak erosion wear rate and angle limits as a function of particle size: circles for aluminum and triangles for Pyrex glass.[11]

For Al between particle size from 100 to 780 μm the erosion rate was found to be proportional to the square of the diameter of the particle. Apart from the fluid mechanics changes described above the dependence on particle size is ascribed to a reduction in energy requirement to form debris particles. Thus there is no fundamental change in the erosion mechanism with the variation in particle size. For sizes below 100 μm there is a transition in erosion mode from direct particle impact to wet abrasion as particles become trapped at the target surface by the squeeze film. For Pyrex glass the dependence was to the fourth power of particle diameter in the particle diameter range of 390 to 780 μm.

3.2 Particle Impact Angle

There is a lot of difference in the response of ductile and brittle materials when the weight loss in erosion is measured as a function of angle of impact. This is well seen in figure 5.
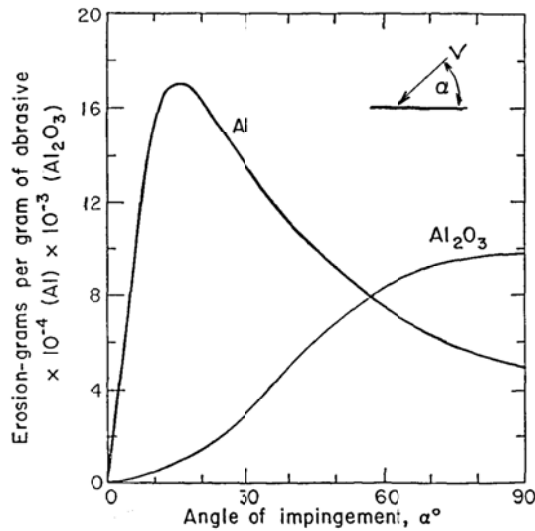

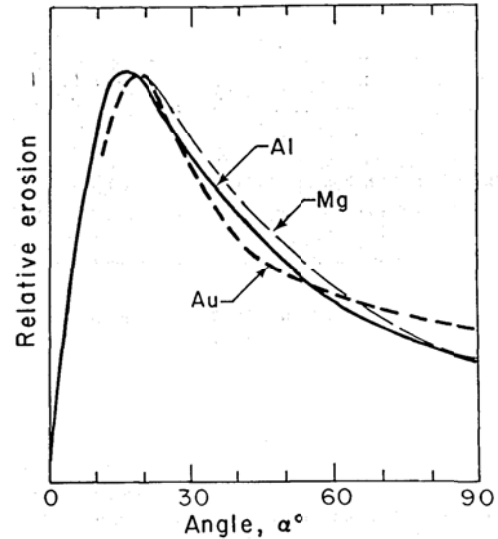Figure 5 Comparison of Al and Al₂O₃ eroded by Sic   127 μm SiC particles [8]

Figure 6 Erosion of Al, Au and Mg by 127μm particles [8]

For ductile behavior the variation in weight loss with the angle of impingement is very similar for materials with widely different thermal and physical properties. This is well shown in figure 6. The similarity of the weight loss curves for materials with widely different properties suggest that not only is the erosion mechanism the same in all cases but also it involves the same physical property i.e. plastic deformation or hardness. The mechanism for erosion for ductile materials is fantastically explained in figure 7 for different angle ranges.

For brittle materials, erosion occurs by propagation and intersection of cracks produced by impinging particles. This mechanism is based on fracture pattern produced when a single particle strikes a smooth surface. Thus its application to highly eroded and fractured surface is questionable, but on comparison with experimental data gives reasonable match.
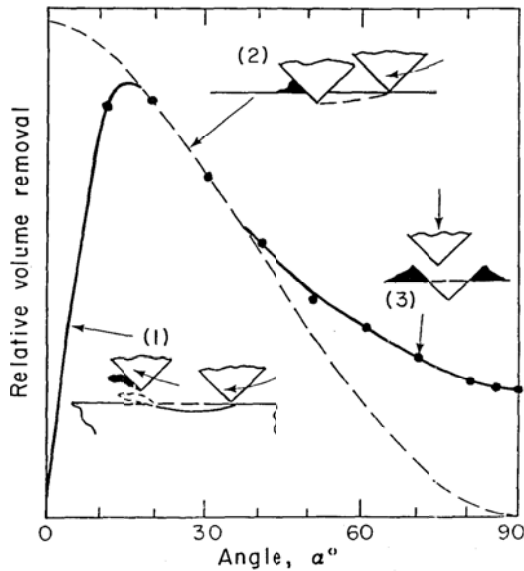
Figure 7 Predicted variation of volume removal with angle curves 1 and 2 and experimental values (curve 3)[8]
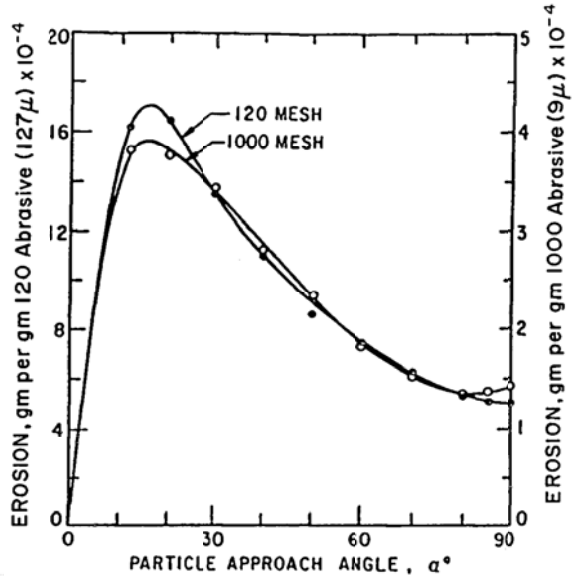
Figure 8 Erosion of 1100-0 Al (Brittle) by 127 µm and 9 µm particles at velocity 152 m/s[8]

3.3 Particle Impact Velocity

As discussed above that with change in particle size there might be some changes in the flow. Figure 9 shows that the amount of erosion damage by small particle is lower than for larger ones for the same impact velocity. The slope is constant though and thus independent of particle diameter.

It is found that the type of particles change the impact velocity dependence of erosion damage. The slope of impact velocity dependence by SiC is larger than that for other particles both for Al and Fe, although the amount of erosion damage was similar, this is well seen in figure 10.
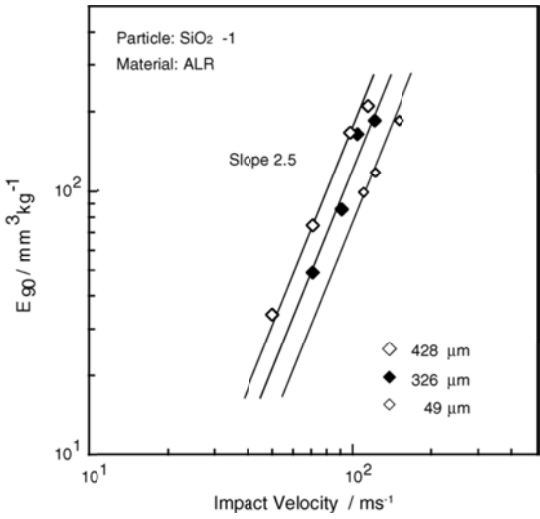

Figure 9 Effects of impact particle diameter on impact velocity dependence on erosion.[16]
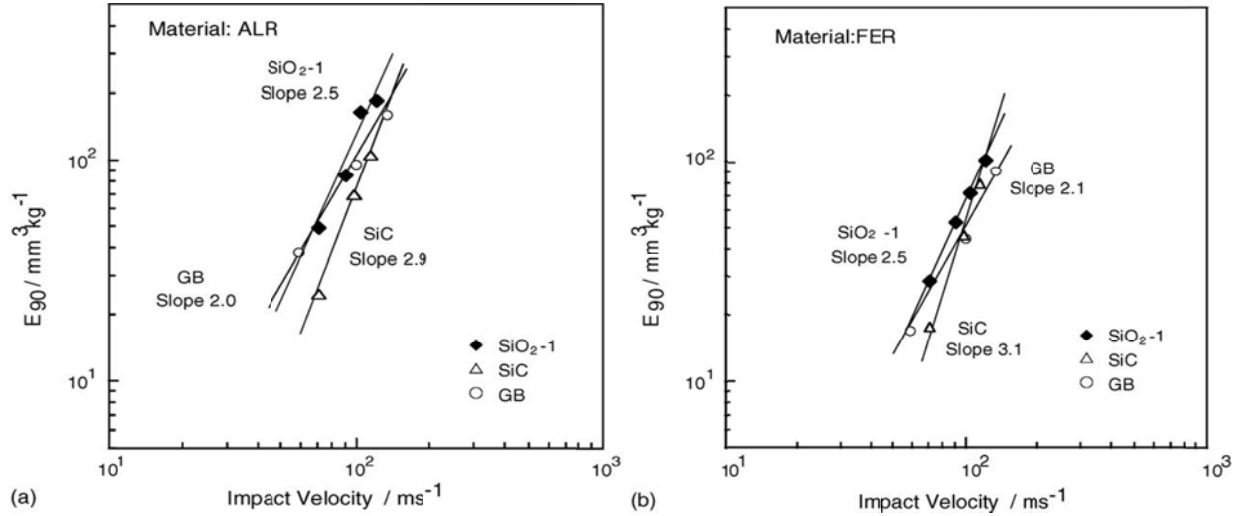
10

Figure 10 Effect of various types of particles on impact dependence of erosion for a) Aluminum (ALR) b) Iron (FER).[16]

3.4 Particle Interference

Here the interference between the stream of incident particles and those rebounding from the surface is considered. The inter-particle collision is considered frictionless and a coefficient of restitution for collision with the surface is assumed. The main principle for this study is that at normal incidence the particle rebounding from the surface interferes with the incident particles, thus causing effective energy transfer to the surface to be reduced.

With the aim to predict the effect of particle interference on the incident power to the surface, a computer model of particle stream in C++ considering scattering by particle surface collisions, effect of friction between the surface and particles, particle scattering by inter-particle collisions was written by Ciampini, Spelt and Papini [13]. The simulations were also capable of account for the effects of incident particle flux, size, velocity, mass and angle of particle stream and stand-off distance.

The model was prepared for all the types of scattering involved:
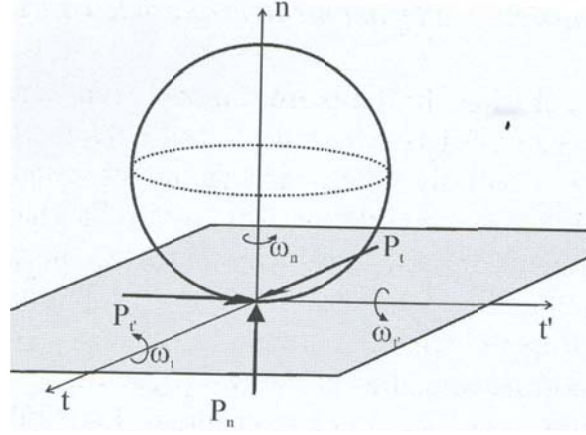
a) For scattering by the surface:

Figure 11 Definition of angular velocities ωᵢ, the impulse Pᵢ in three coordinate directions n,t and t'.[13]

Model equations for particle sliding through the impact:

$$V_n = -e_{ps} v_n \tag{12}$$

$$V_t = -\mu_t v_n (1 + e_{ps}) + v_t \tag{13}$$

$$V_t = -\mu_t v_n (1 + e_{ps}) + v_t \tag{14}$$

$$\Omega_t = \omega_t - \frac{5}{2r_p} \mu_t v_n (1 + e_{ps}) \tag{15}$$

$$\Omega_{t'} = \omega_{t'} - \frac{5}{2r_p} \mu_{t'} v_n (1 + e_{ps}) \tag{16}$$

where V and v are the incident and rebound velocities, t and t' are directions as shown in figure, e_ps is coefficient of restitution and μ is the impulse ration in a particular direction.

For the case where sliding end prior to the contact we replace by

$$V_t = r_p \Omega_{t'}$$
<div align="right">(17)</div>

$$V_{t'} = r_p \Omega_t$$
<div align="right">(18)</div>

b) Effect of friction:

$$\mu^2 = \mu_t^2 + \mu_{t'}^2$$
<div align="right">(19)</div>

c) Scattering by inter-particle collisions:

$$V_{n1} = \frac{m_2\left[v_{n2} + e_{pp}(v_{n2} - v_{n1})\right] + m_1 v_{n1}}{m_1 + m_2}$$
<div align="right">(20)</div>

$$V_{n2} = \frac{m_1\left[v_{n1} - e_{pp}(v_{n2} - v_{n1})\right] + m_2 v_{n2}}{m_1 + m_2}$$
<div align="right">(21)</div>

where v_{n1} and v_{n2} are components of incident particle velocities normal to the common point and V_{n1} and V_{n2} final velocities in the same directions.

However, there are not many experimental studies directed to particle interference, Shipway and Hutchings devised a method to experimentally determine the minimum particle flux at which particle-particle interactions become significant. The critical flux of three sizes of spheres was determined from the experimental study, together with the predictions from the present the simulations are compared in table 1.[26]

Table 1
Critical flux for negligible particle interactions: measured (from [15]) and predicted (from present simulation)

Sphere diameter (μm)	Range of flux in which critical flux lies [15] (kg s^{-1} m^{-2})	Predicted critical flux (kg s^{-1} m^{-2})
69	0–0.4	0.07
231	0.76–2.9	0.9
700	0.6–2.9	8.0

4. Fluid Effects

The effect of particle on the impinging surface carried by a fluid depends greatly on the fluid flow. The fluid factors which affect erosion are state of flow (laminar or turbulent), velocity, temperature and chemical and physical properties. These factors change the dynamic conditions of the particle approaching the surface which in turn affect the wear in manner discussed below. Thus, it can be said that for accurate study of erosion by solid particle, the fluid motion should be studied accurately. As is it this fluid motion which eventually determines impact angle, velocity, flux, interference, fragmentation etc.

Flows wherein suspended particles interact are not limited to the situations involving direct physical contact of the particles. Situations arise in which even though, while they do not collide, the particles are sufficiently numerous to affect one another through collective influence through the fluid. The question of averaging arise in relation to continuum (Eulerian) formulations of two phase flow transport equations or discrete (Lagrangian) theoretical descriptions of particle laden flows. In this respect we can relate our consideration with the CFD model used by Min-Hua Wang, Cunkui Huang and Nandakumar for particle tracking and turbulence dispersion [25].

4.1 Particle Tracking

Lagrangian particle tracking is used to calculate the trajectory by integrating the force balance on the particle that relates the rate of velocity change

$$M_p \frac{du}{dt} = F = F_D + F_A + F_B \tag{22}$$

where, M_p is the particle mass and F is the overall force on the particle including drag force F_D, added mass force F_A, and buoyant force F_B. Drag force is the major component of the force on the particle and is given as:

14

$$F_D = \frac{1}{2}\pi d^2 \rho C_D |V_R| V_R \qquad (23)$$

where

$$C_D = 24\left(1 + 0.15\,\mathrm{Re}^{0.687}\right)/\mathrm{Re} \qquad (24)$$

here C_D is the coefficient of discharge, Re is Reynolds's number, d is the diameter of the particle, μ and ρ are the density and viscosity of continuous phase and V_R is the relative velocity of two phase.

The added mass is given by:

$$F_A = -\frac{1}{12}\pi d^3 \rho \frac{du}{dt} \qquad (25)$$

and the buoyant force is

$$F_B = \frac{1}{6}\pi d^3 (\rho_P - \rho)g \qquad (26)$$

where ρ_P is particle density and g is acceleration due to gravity.

4.2 Turbulence Dispersion

The effect of turbulence on the particle trajectories have been accounted for in model by Gosman and Loannides[17]. The turbulence of the particle motion is introduced due to interaction of particle with random motion of turbulent fluid eddies. The characteristic lifetime of an eddy is given by:

$$t_e = 1.5^{1/2} C_\mu^{3/4} \frac{k}{\varepsilon} \qquad (27)$$

And the eddy length is given as:

$$I_e = C_\mu^{3/4} \frac{k^{3/2}}{\varepsilon}$$

(28)

where, c_μ is turbulence model constant. k, ε are predicted quantities.

5. Erosion-corrosion

Erosion-corrosion of materials in slurry environments is a complex phenomenon, which is dependent on a wide range of parameters relating to the tribological contact – particle/target properties – and the nature of environment. Erosion may enhance corrosion by removal of a passive film 'additive' effect as the corrosion loss may be readily computed Faraday's Law. Corrosion may enhance the erosion rate through preferential dissolution in a two phase material and this is the so called 'synergetic' effect. Corrosion may also inhibit erosion through formation of a passive film – 'antagonistic' effect.

A significant method for understanding the mechanism is through identification of regimes of behavior using quantitative techniques. Here the concept of erosion corrosion maps comes handy. Such maps identify the regimes of interaction, depending on relative contributions of the corrosion and erosion rates and the nature of corrosion process i.e. whether active dissolution, where metal dissolves, or passivation, where an adherent film forms on the surface.

In the initial work mathematical models were generated combining the effects of solid particle erosion with those of aqueous corrosion. The model was created to address wide range of variables involved through eight dimensionless groups incorporating twelve variables. But there is no point going over this model in detail as the prime assumption is that the erosion-corrosion is 'additive' and neglects the so called 'synergistic' effect.

Here a model by Stack and Jana[23][24] is discussed where the synergistic effect is considered.

The relationship between erosion and corrosion is defined as:

$$K_{ec} = K_e + K_c \qquad (29)$$

$$K_e = K_{eo} + \Delta K_c \qquad (30)$$

$$K_c = K_{co} + \Delta K_c \qquad (31)$$

where K_e is total erosion rate, K_c is total corrosion rate, K_{ec} is overall erosion-corrosion rate, K_{eo} erosion rate in absence of corrosion, ΔK_e is the change in erosion rate due to corrosion, K_{co} is the corrosion rate in absence of erosion and ΔK_c is the change in corrosion rate due to erosion.

It is assumed that in active region, there is no enhancement in corrosion due to erosion in passive region. Also, the enhancement in corrosion due to successive formation and removal of film is significantly greater that the corrosion in absence of erosion. Thus in active region:

$$K_e = K_{eo} \qquad (32)$$

$$K_c = K_{co} \qquad (33)$$

In passive region:

$$K_e = \Delta K_c \qquad (34)$$

$$K_c = \Delta K_c \qquad (35)$$

Hence the model gives the values as:

$$K_c = k_1 \times 10^{-4} i_{anet} \qquad (36)$$

where k_1 is tabulated in , i_{anet} is net anodic current density.

17

$$K_e = \frac{0.65 D_p^{0.25} c v^{3.5}}{C_p T_m^{0.75} H_s^{0.25}} \tag{37}$$

where D_p is particle density, c is particle concentration, v is particle velocity, C_p specific heat of target, T_m is melting point of target and H_s is static hardness of target.

$$\Delta K_c = \frac{k_3 D_f h c v^2}{r D_p^{0.5} H_s^{0.5}} \tag{38}$$

where k_3 is tabulated in , D_f density of passive film and h thickness of passive film.

From the results cited in [22], it is found that flow velocity v is the leading factor driving synergistic damage and the next important factor is particle ejection rate. But from the results cited in [23], where more intense work is done for construction of erosion-corrosion maps for various metals, significant differences as seen for different metals.

Initially Stack and Jana considered the effect of ph and applied potential [23] but later it was found and the effect of impact angle was also studied [24].

It is seen from the results that the maps for pure metals like Nickel, Copper and Aluminium exhibit vast differences compared to Iron. Figure 12, 13.
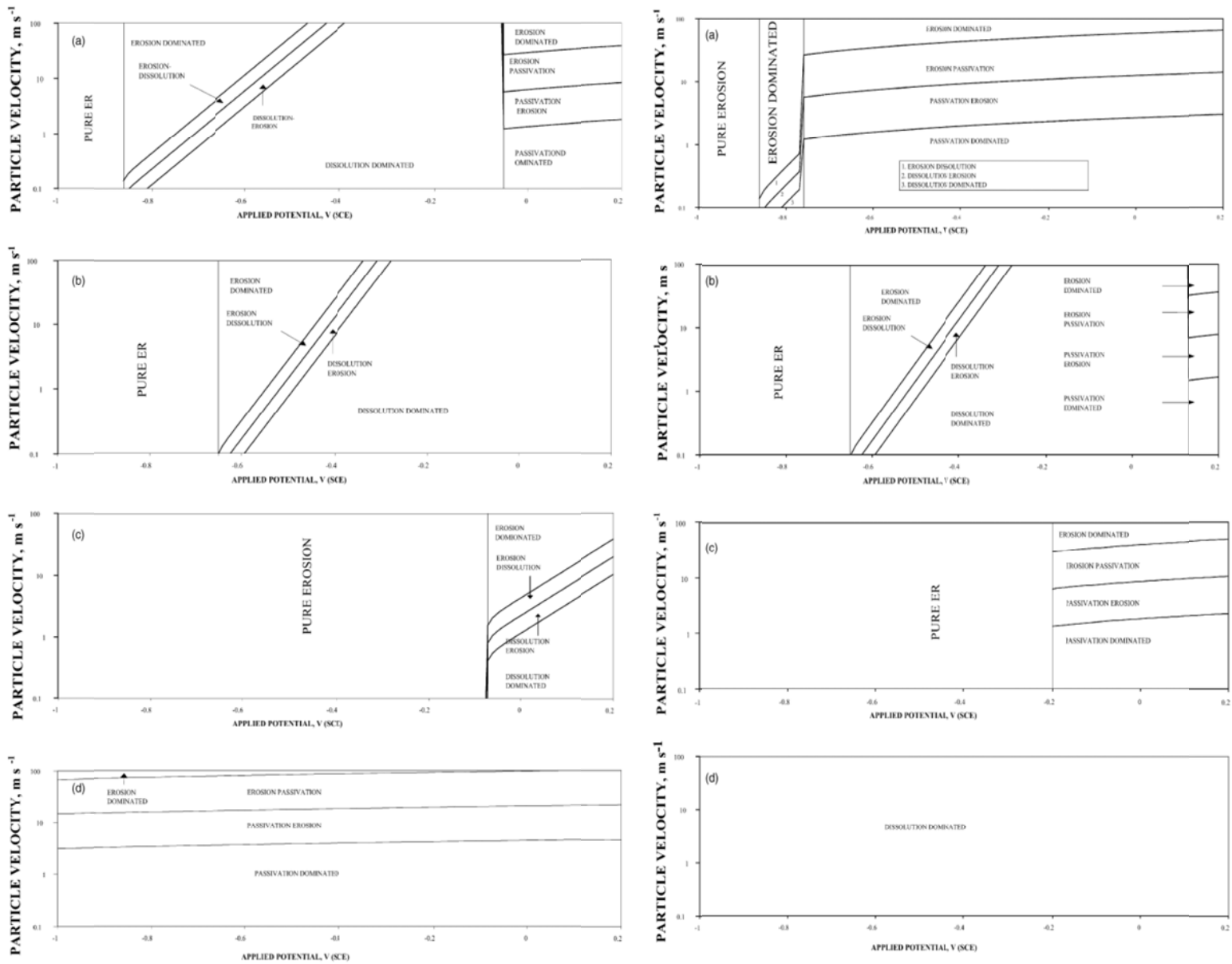
Figure 12 Particle velocity – applied potential maps for pH 5 (left) and pH 9 (right): a) Fe b) Ni c) Cu and d) Al [23]
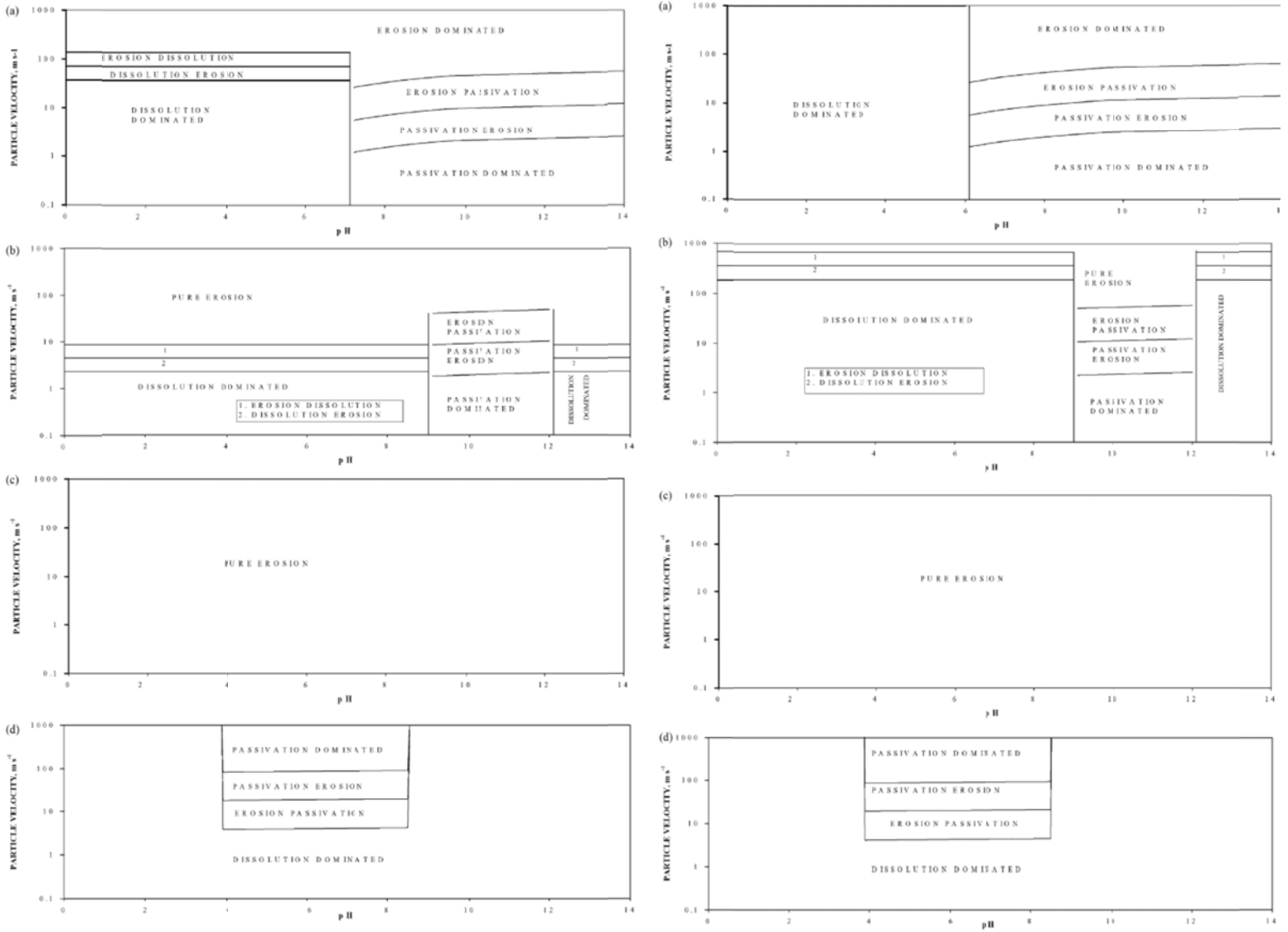
Figure 13 Particle velocity – pH maps at -0.45V (left) and -0.26V (right): a) Fe b) Ni c) Cu and d) Al [23]

It can be seen in figure 12 that for Ni the dissolution affected extends to a much higher potential than for Fe. Cu by contrast exhibits behavior almost entirely dominated by mechanical process. From figure 13 it can be seen that the pH at which passivation occurs shifts to higher values as applied potential increases for Ni. However, the actual corrosion is rate than for Fe in the dissolution affected region. For Cu wastage is purely based on mechanical process. The map for Al is dominated by a passivation affected region at intermediate pHs, with the surrounding areas at high and low pH values affected by dissolution.
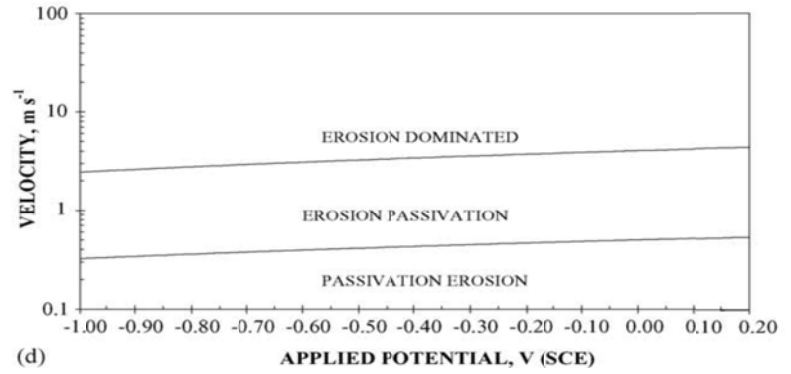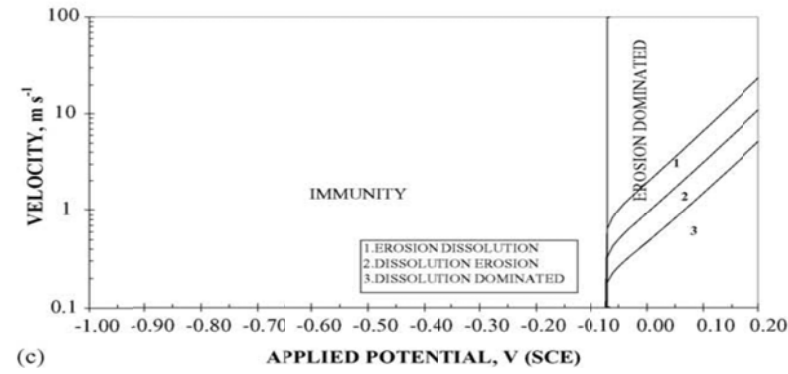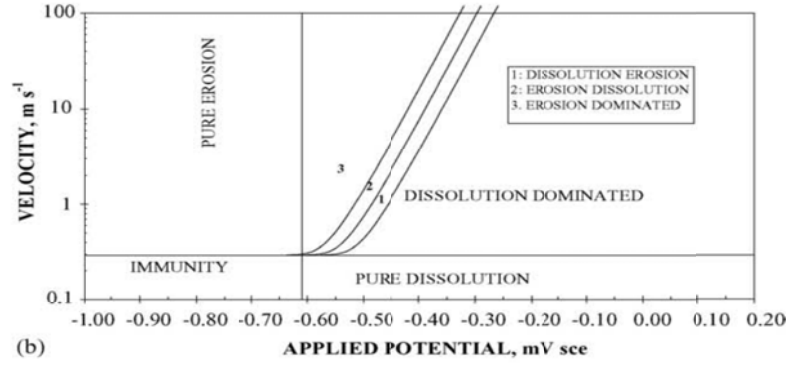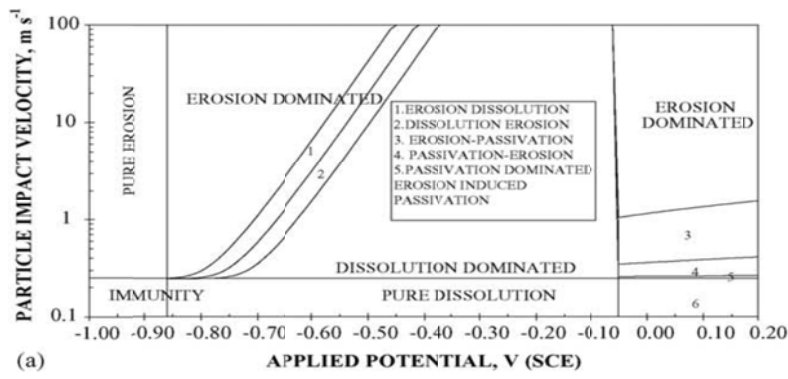
20

Figure 14 Particle velocity – pH maps for 10° impact angle at pH 5: a) Fe b) Ni c) Cu and d) Al [24]
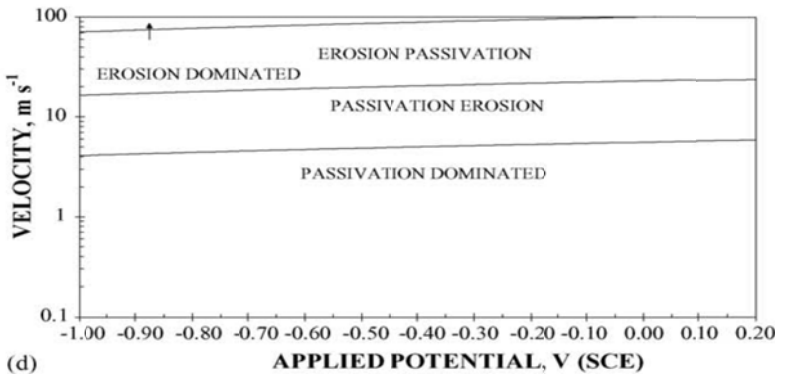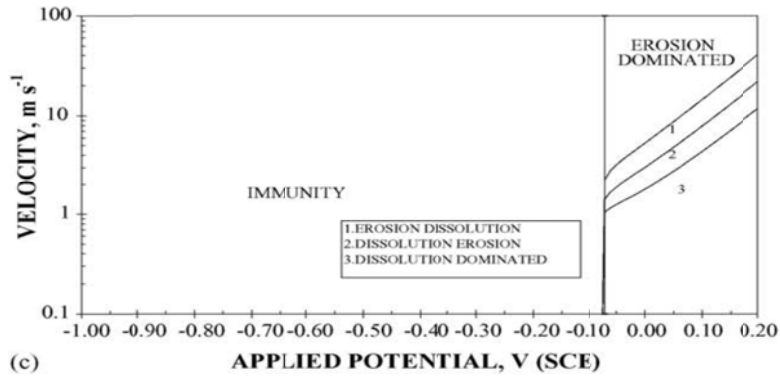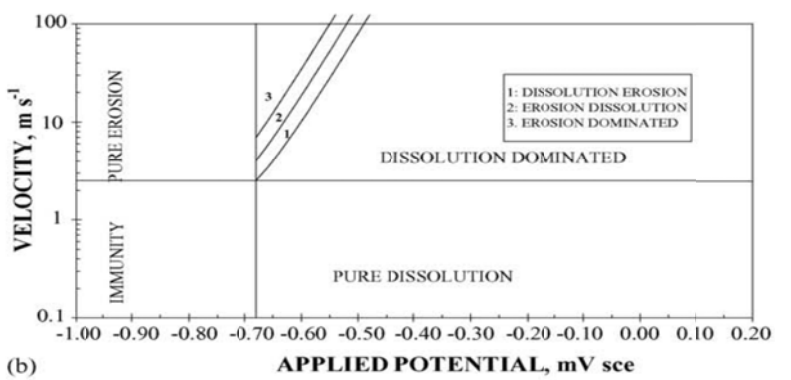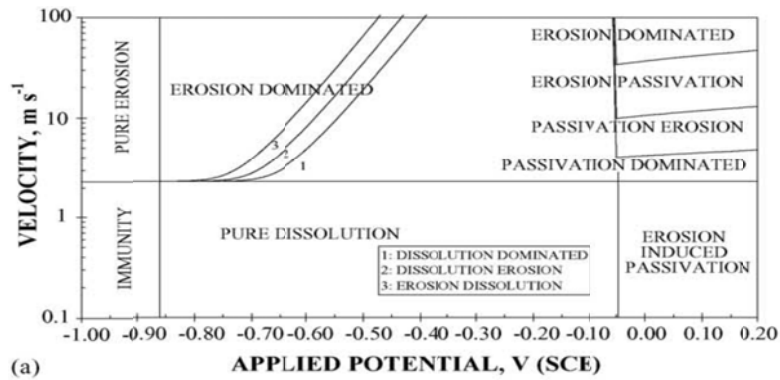

Figure 15 Particle velocity – pH maps for 90° impact angle at pH 5: a) Fe b) Ni c) Cu and d) Al [24]

Figure 14 and 15 above shows the effect of impact angle on erosion-corrosion regime. It is seen that Ni shows higher dissolution affected region than Fe and shows no passivation region except at pH 9. The passivation potential for Ni is much higher that for Fe and not within the range, but at pH 9 the passivation potential reduces to 0.13V. the reason for this transition to pure dissolution at higher velocities at normal compared to oblique impacts for Fe and Ni is due to lower erosion rates at such impact angles. It also shows that for Cu the immune zone is largest and hence mechanical ersion process is the main cause of degradation, except for at higher potentials.

6. Material Issues

Mainly the materials used for constructing the models and for experimentation are various types of steels, copper or aluminum which generally comprise for ductile materials and glass, cast iron which form in the brittle group. Also, for material test in which materials like graphite, perspex were used for the group of neither brittle nor ductile.
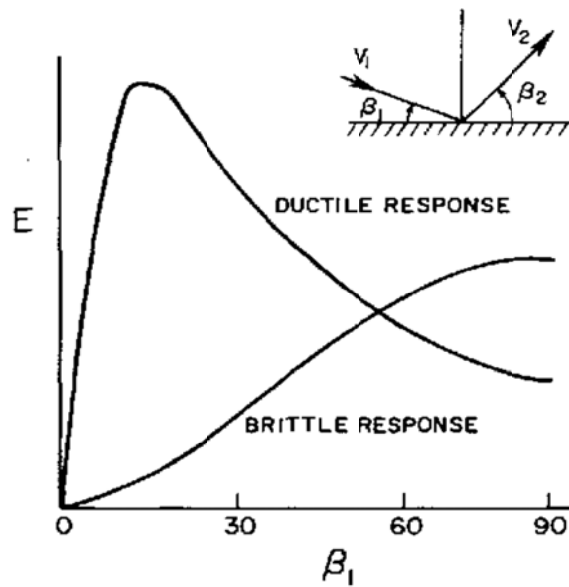

Figure 16 Typical erosion curves for ductile and brittle materials [18].

The experiments were mainly carried out with various heat-treated steels, which is not the best choice of materials. The main reason for this is the nature of steels, their complex microstructures and the possible presence of residual stresses. Also, the presence of relatively coarse carbides in the microstructure may cause voids and cracks to form even under compressive stress generally found in the deformation zone during erosion. Due to this, delamination might occur resulting in thick chunks rather than thin extruded platelets.

It is also seen that material hardness plays a dominant role in the process of erosion. Measurements of volume removal in erosion as a function of Vickers hardness is shown in figure 17. It is seen that annealed metals show a volume removal inversely proportional to the Vickers hardness. Expression relating erosion to impact velocity and impact angle are dependent on the hardness on the material, and researchers say that hardness should be a dependent variable for their predictive equations.
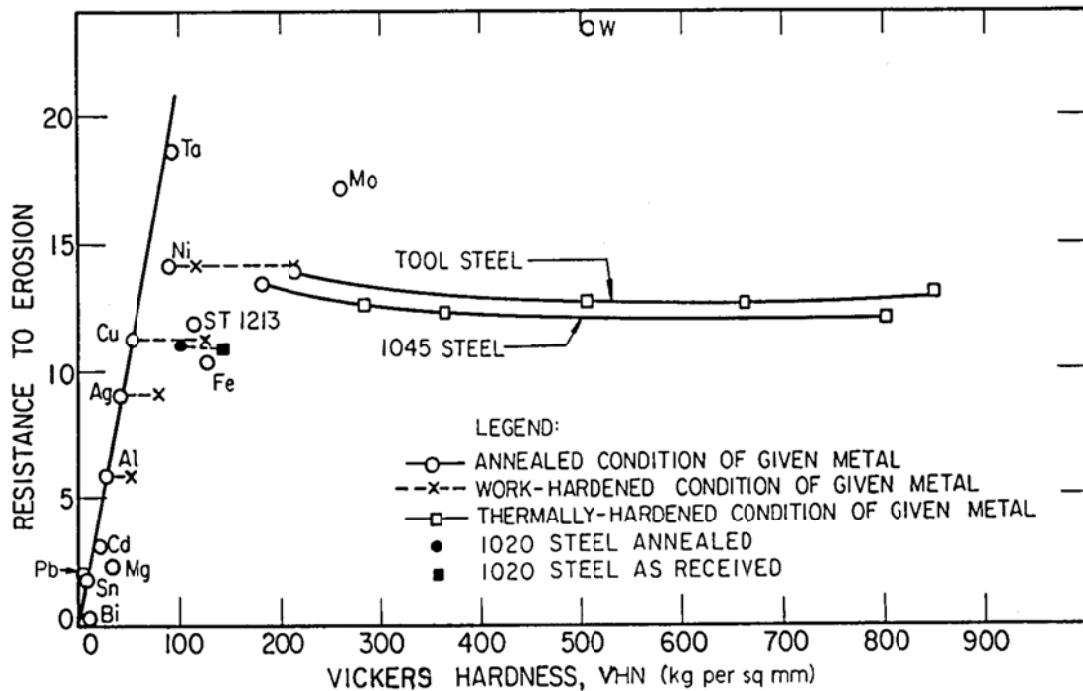

Figure 17 Resistance to erosion as a function of VHN of the materials before erosion [8].

As discussed that erosion-corrosion is a complex phenomenon, especially corrosion is highly affect by the materials on which it is acted upon. The synergistic effect for some of the materials is very straight forward, like preferential dissolution of the γ matrix for high Cr steels, obtained by slow solidification process was associated with depletion of Cr from the matrix. This resulted in a significant increase in the overall erosion-corrosion rate compared with that for same alloy formed by rapid solidification.

Trying to generalize the materials influence:

In case of passsivating materials, the synergistic effect is mainly attributed due to mechanical removal of the protective layer by particle impact.

In case of actively corroding materials, the specific mechano-chemical effect is related to the plasticization of the material, affecting its activity through variations in metal density and grain defectivity.

Thus, it can be said that synergism weight loss is mainly dominated by the chemical composition of the material and not by its mechanical properties.

7. Open Issues

Though, work related to the field of erosive wear is going since more than half century, during which ingenious solutions have been devised for many practical erosion problems, however, the fundamental mechanism is yet not fully explored. The models may discuss platelet removal mechanisms or cutting and ploughing mechanism, but the precise understanding of local deformation and fracture process involved is still not completely described.

Even if till date work is considered, every model or result involves assumptions for many of the principal factors affecting this complicated phenomenon of erosion. Table 2 [8] states principal factors which influence erosion.

Table 2

Factors which influence erosion in an inert environment

Fluid flow conditions
Angle of impingement Particle velocity Particle rotation Particle concentration in the fluid Nature of the fluid and its temperature

Particle properties
Size Shape Hardness Strength (resistance to Fragmentation)

Surface properties
Stress as a function of strain, strain-rate and temperature Hardness Fracture toughness Stress level and residual stress Shape Microstructure (composites) (fatigue, melting point, etc.)

Assumptions are put on most of these factors to simplify the calculations, depending on the relative importance for particular application studied. The effects these assumptions have on the results are in itself open issues yet to be addressed, some of which are discussed below:

a) All models assume that mechanism predicted by the interaction of the particle with a smooth surface. But in reality, after some initial time the impact is no longer with a smooth surface but with eroded surface. This may change the interaction with the surface as the surface properties change along with the microstructure at the surface. This may induce some errors in the results of the model or simulations.

b) It is also assumed that all the particles are of identical shape and radius, which is very hard to obtain in reality. The effects of change in particle dimensions are directly on flow conditions, velocity distribution in the flow, distribution of particle impact angles and impact frequency. These may introduce errors in the results.

c) It is practically impossible define a fixed shape during study of effect by angular particles. But when cutting model is considered shape and orientation at which particle strikes the surface heavily affects deformation and friction that occurs during material removal process. Effect of particle rotation can also be attributed to the same effects.

d) The velocity distribution across the nozzle is assumed to be constant. But in actual velocity of the particles exiting a standard round nozzle will be greatest

at the center and lower at the edges. This has infects on the inter-particle interference and also the force transfer during the impact at the target surface.

e) Effect of strain-hardening is also neglected, but as more and more particle strike the surface, the surface get strain hardened due to plastic deformation occurring on the surface. This will result in more particles required to remove material from the surface.

f) It is assumed that the adhesion of the oxide film is constant for all metals discussed in erosion-corrosion above. But in practice oxides which from on the metallic materials may be porous and adhered loosely with different properties for different materials.

No fundamental experimental study of erosion by particle impact has yet been successfully done in which the characteristics of turbulence are varied in a controlled and systematic manner. Conducting such investigations is imperative, as it can provide data necessary for guiding and testing mathematical model development that will help predict erosive wear to a great extent.

8. Conclusion

To conclude we can re-quote what Wahl and Harstien said in their technical paper more than 50 years back, that "In all areas of erosive wear mentioned here, there are still considerable contradictions and gaps in our knowledge".

References

1. Iain Finnie Erosion of surfaces by solid particles (1960).
2. J.G.A. Bitter A study of erosion phenomena Part 1 (1963)
3. J.G.A. Bitter A study of erosion phenomena Part 2 (1963)
4. J.H. Neilson, A. Gilchrist Erosion by a stream of solid particles (1968)
5. I.M. Hutchings A model for the erosion of metals by spherical particles at normal incidence (1980)
6. G. Sundararajan A comprehensive model of solid particle erosion of ductile materials (1991)
7. M.S. Bingley, D.J. O'Flynn Examination and comparison or various erosive wear models (2004)
8. Iain Finnie Some reflections on past and future of erosion (1995)
9. F.G. Hammitt, J.B. Hwang, Linh N. Do Interrupted jet water gun impact-erosion studies on metallic alloys (1974)
10. M.T. Benchaita, P. Griffith, E. Rabinowicz Erosion of metallic plate by solid particles entrained in a liquid jet (1983)
11. H.M. Clark, Ryan B. Hartwich A re-examination of the 'particle size effect' in slurry erosion (2001)
12. H.M. Hawthrone, Y. Xie, S.K. Yick A study of single particle-target surface interactions along a specimen in Coriolis slurry erosion tester (2002)
13. D. Ciampini, J.K. Spelt, M. Papini Simulation and interference effects in particle streams following impact with a flat surface Part 1 Theory and analysis (2003)
14. D. Ciampini, J.K. Spelt, M. Papini Simulation and interference effects in particle streams following impact with a flat surface Part 2 Parametric study and implications for erosion testing and blast cleaning (2003)
15. Y.I. Oka, K. Okamura, T. Yoshida Particle estimation of erosion damage caused by solid particle impact Part 1 Effects of impact parameters on a predictive equation (2005)
16. Y.I. Oka, T. Yoshida Particle estimation of erosion damage caused by solid particle impact Part 2 Mechanical properties of materials directly associated with erosion damage (2005)
17. A.D. Gosman, E. Ioannides Aspects of computer simulation of liquid fuelled combustors (1981)
18. J.A.C. Humphery Fundamentals of fluid motion on erosion by solid particle impact (1990)
19. M. Gustavsson Fluid dynamic mechanisms of particle flow causing ductile and brittle erosion (2002)
20. N.K. Bourne On stress wave interactions on liquid impacts (2004)
21. M.M. Stack, N. Corlett, S. Turgoose Some recent advances in the development of theoretical approaches for the construction of erosion-corrosion maps in aqueous conditions (1999)
22. Benedetto Bozzini, Marco E. Ricotti, Marco Boniardi, Claudio Mele Evaluation of erosion-corrosion in multiphase flow via CFD and experimental analysis (2003)
23. M.M. Stack, B.D. Jana Modelling particulate erosion-corrosion in aqueous slurries: some views on construction of erosion-corrosion maps for a range of pure metals (2004)
24. M.M. Stack, B.D. Jana Modelling impact angle effects on erosion-corrosion of pure metals: construction of materials performance maps (2005)
25. Min-Hua Wang, Cunkui Huang, K. Nandakumar, P. Minev, J. Luo, S. Chiovelli Computational fluid dynamics modeling and experimental study or erosion in slurry jet flows (2009)

26. P.H. Shipway, I.M. Hutchings A method for optimizing the particle flux in erosion testing with a gas-blast apparatus (1994)

27. H. Wahl, F. Hartstein, translated into English, January 1979 for Lawrence Livermore National Lab.,UCRL Translation 11447